ACS APPLIED MATERIALS & INTERFACES

Research Article

www.acsami.org

Hydrophobic Antifouling Electrospun Mats from Zwitterionic Amphiphilic Copolymers

Sefika Ozcan,[†,‡] Papatya Kaner,[†] David Thomas,[§] Peggy Cebe,[§] and Ayse Asatekin*[,†]

[†]Department of Chemical and Biological Engineering, Tufts University, 4 Colby Street, Medford, Massachusetts 02155, United States

[‡]Department of Polymer Science and Technology, Middle East Technical University, 06800 Ankara, Turkey

[§]Department of Physics and Astronomy, Tufts University, 574 Boston Avenue, Medford, Massachusetts 02155, United States

Supporting Information

ABSTRACT: A porous material that is both hydrophobic and fouling-resistant is needed in many applications, such as water purification by membrane distillation. In this work, we take a novel approach to fabricating such membranes. Using the zwitterionic amphiphilic copolymer poly(trifluoroethyl methacrylate-*random*-sulfobetaine methacrylate), we electrospin nonwoven, porous membranes that combine high hydrophobicity with resistance to protein adsorption. By changing the electrospinning parameters and the solution composition, membranes can be prepared with a wide range of fiber morphologies including beaded, bead-free, wrinkly, and ribbonlike fibers, with diameters ranging between ∼150 nm and 1.5 μm. The addition of LiCl to the spinning solution not only helps control the fiber morphology but also increases the segregation of zwitterionic groups on the membrane surface. The resultant electrospun membranes are highly porous and very hydrophobic, yet resist the adsorption of proteins and retain a high contact angle (∼140°) even after exposure to a protein solution. This makes these materials promising candidates for the membrane distillation of contaminated wastewater streams and as self-cleaning materials.

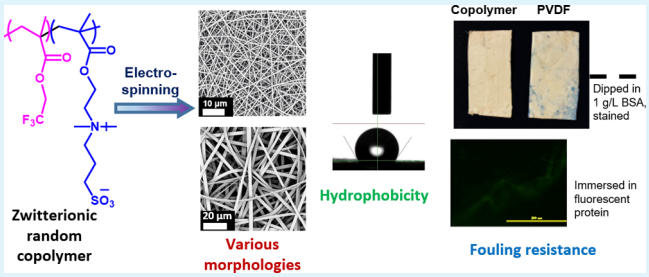

KEYWORDS: *electrospinning, zwitterion, polymer, protein adsorption, fouling resistance*

1. INTRODUCTION

The adsorption of proteins and other biomolecules on surfaces is a crucial challenge in many fields. In membrane filtration applications for water treatment, this phenomenon is the main cause of fouling that leads to a severe flux decline. Fouling also leads to problems in medical applications (e.g., implants, wound dressings, surgical equipment, and protective apparel), marine and architectural surfaces, and biosensors.[1] The formation of an adsorbed layer of proteins and other macromolecules on porous materials can be especially problematic because of the large surface area involved, leading to pore narrowing and changes in surface chemistry, wettability, and other properties that strongly affect the performance. This layer can also enable and enhance the adhesion of cells and microorganisms on the surface, serving as the first step in the formation of a biofilm.

To address these concerns, surfaces that strongly resist protein adsorption and cell adhesion have been the focus of much research.[1−7] Protein adsorption on hydrophobic surfaces can more significantly decrease the interfacial energy. This implies that in general, hydrophilic surfaces tend to foul less than hydrophobic ones. Indeed, hydrophilicity is listed as a key criterion for surfaces that resist protein adsorption, along with the presence of hydrogen-bond acceptors, lack of hydrogen-bond donors, and being neutral in charge.[3]

A few studies, however, have shown that surfaces that combine small patches of hydrophilic and hydrophobic materials can resist fouling. Specifically, amphiphilic surfaces, with compositional heterogeneities on the length scale of the foulant, may discourage thermodynamically favorable interactions between the foulant and the surface, thus limiting the adsorption.[1,8−11] Such a surface may be hydrophobic on average, exhibiting a sessile drop water contact angle (CA) above 90°, but still resists fouling. However, these studies are preliminary and almost exclusively focused on roughly flat surfaces.

There is still a significant need for porous materials that are both fouling-resistant and hydrophobic. One important application is membrane distillation (MD), which utilizes a hydrophobic porous membrane that separates the liquid phase on the one side from the vapor phase on the other. Water vapor can diffuse through the membrane, whereas the liquid, along with nonvolatile solutes (e.g., salt and organic molecules), is retained.[12] MD is often used for treating highly contaminated water and wastewater streams, containing both high salt concentrations and large quantities of organic macromolecules

Received: February 25, 2018
Accepted: April 16, 2018
Published: April 16, 2018

DOI: 10.1021/acsami.8b03268
ACS Appl. Mater. Interfaces XXXX, XXX, XXX−XXX

and/or oil.[13] The adsorption of these organic foulants on the membrane surface during operation makes the membrane surface more hydrophilic, which eventually allows the breakthrough of the wastewater to the permeate side. This leads to a drastic decrease in the effluent quality and efficiency of the operation.[14] In most applications, fouling is prevented by making the membrane surface more hydrophilic.[1,15] However, a successful MD membrane has to be hydrophobic and must maintain its high CA even upon exposure to foulants.[14,16]

Electrospinning is an easy and robust method for producing nanometer to micrometer scale fibers from many polymers. The fibers and the nonwoven materials have been used in a wide variety of applications, from photocatalysis[17] to drug delivery[18,19] and tissue engineering[20,21] to water remediation.[12,22−24] Electrospinning can generate membranes and nonwoven materials with extremely high porosity, highly interconnected pores, controllable phase structure (crystalline, rigid amorphous, and mobile amorphous phases[25−30]), and controlled pore size and fiber diameter.[31−33] These are crucial advantages for many membrane applications. In MD applications, the high porosity and the interconnected pore structure of electrospun materials lead to a high flux and thermally efficient membranes.[12] To achieve high hydrophobicity, most electrospun MD membranes are made of fluorinated polymers, especially poly(vinylidene fluoride) (PVDF) and its derivatives.[12]

Therefore, in this study we aim to create highly hydrophobic and porous fiber mats that resist fouling, by electrospinning a novel material that combines hydrophobic groups with fouling-resistant groups. We selected zwitterions, defined as groups that contain equal numbers of anionic and cationic moieties linked by covalent bonds, as the fouling-resistant functionalities. The performance of zwitterions is comparable to the best known systems for resisting protein adsorption[2,34−37] and bacterial adhesion,[34,35] with the fouling resistance attributed to the very small perturbation effect at the polymer−water interface.[36,38] This makes them especially promising for preventing fouling in a wide range of systems, including membranes.[6,7,39−43]

The unusual properties of zwitterionic groups such as their strong dipole moments, high hydrophilicity, and interesting interaction with salt ions[44] may lead to novel outcomes in the electrospinning process. Yet, there are very few reports of the electrospinning of zwitterion-containing polymers in the literature. Homopolymers of the zwitterionic monomer sulfobetaine methacrylate (SBMA) can be formed into nanofibers by electrospinning,[45] but these fibers will extensively swell and eventually dissolve in water unless cross-linked.[46,47]

Amphiphilic copolymers that combine a zwitterionic monomer with a hydrophobic monomer can lead to better stability and higher hydrophobicity, yet there are few reports on the electrospinning of such copolymers in the literature.[42,48−51] One team described lower protein adsorption and thrombogenic activity in thin films of polyurethanes functionalized with sulfobetaine groups.[49] They also mentioned that they prepared electrospun mats and tubes, but also admitted that the electrospinning process requires more study. Another team has reported the electrospinning of random copolymers of poly(butyl methacrylate) and SBMA (PBMA-*r*-SBMA).[48] This study has shown that these copolymers can be electrospun at lower polymer concentrations, and the addition of salts can improve the morphology of the nonwoven mats by preventing the formation of beads along the fibers. However, applications or surface properties of these materials were not discussed. Electrospun mats have been prepared from terpolymers of butyl methacrylate with another zwitterionic mononomer (methacryloxyphosphorylcholine) and a cross-linkable monomer,[51] with a focus on the prevention of protein and platelet adsorptions. Zwitterion-containing mats were unstable in water, which is why the ultraviolet-cross-linkable monomer was included. A terpolymer of SBMA with methyl methacrylate and *n*-hexyl methacrylate was also studied for its applications as a biomaterial, both as flat films and as electrospun mats.[52] The high glass transition temperature of the copolymer in the absence of water enabled the successful electrospinning of fibers. However, when immersed in water, these mats were heavily plasticized and swelled to the point of losing integrity.

The poor mechanical properties of these materials in water arise from the low glass transition temperature, T_g, of their hydrophobic polymer segments. In all these materials, the zwitterions interact with each other to act as physical cross-links.[53] When exposed to water, these cross-links are broken, leading to swelling and softening of the fibers. If T_g of the hydrophobic sections of the polymer is above rather than below the room temperature, this would likely improve the stability of the resultant nanofibers in water. Indeed, electrospun mats prepared from the random copolymer poly(methyl methacrylate-*random*-carboxybetaine methacrylate) (PMMA-*r*-CBMA) were stable enough in water for extensive testing during exposure to aqueous media, including tests for biocompatibility and for use as a wound-dressing material.[50] T_g of PMMA is around 100 °C, so it remains rigid and intact even when the zwitterionic CBMA domains are heavily plasticized in water. This study, however, did not focus on the electrospinning process and the effect of the electrospinning process on the morphology or surface chemistry of the materials obtained.

Recently, we reported the formation of electrospun membranes from blends of PVDF with random copolymers of methyl methacrylate with two zwitterionic monomers, SBMA and sulfobetaine-2-vinyl pyridine.[42] This study showed that electrospun mats could be obtained from blends containing up to 15−20 wt % of the zwitterionic copolymer and that these mats are hydrophobic but resist protein adsorption. The pure zwitterionic copolymers were not electrospun in this study, however, because the copolymers were being investigated specifically as surface-modifying agents to prevent fouling.[6]

Here, we report the formation and properties of electrospun membranes prepared from a random amphiphilic copolymer of a fluorinated monomer, 2,2,2-trifluoroethyl methacrylate (TFEMA), with ∼20 wt % of the zwitterionic monomer SBMA. Electrospun membranes can be prepared with a wide range of morphologies, with fiber size ranging between ∼200 nm and 3 μm. Beaded, bead-free, wrinkly, and ribbonlike merged fibers can be formed by changing the solution composition and electrospinning parameters. The addition of lithium chloride (LiCl) to the spinning solution not only helps control the fiber morphology but also increases the segregation of zwitterionic groups on the membrane surface. The resultant electrospun membranes are highly porous and very hydrophobic, yet resist the adsorption of proteins and retain a high CA even after exposure to a protein solution. This makes these materials very promising for MD of contaminated wastewater streams and as self-cleaning materials.

DOI: 10.1021/acsami.8b03268
ACS Appl. Mater. Interfaces XXXX, XXX, XXX−XXX

Table 1. Solution Compositions and Collectors Used in Preparing Electrospun Materials

	spinning solution composition				
sample code	PTFEMA-*r*-SBMA (g)	LiCl (g)	solvent type	solvent amount (mL)	collector type
P-DMAC	0.18	0	DMAc	1	stationary
P-TFE	0.18	0	TFE	1	stationary
P18-0	0.18	0	3:1 TFE/DMF	1	stationary
P18-0.5	0.18	0.005	3:1 TFE/DMF	1	stationary
P18-1	0.18	0.010	3:1 TFE/DMF	1	stationary
P18-1.5	0.18	0.015	3:1 TFE/DMF	1	stationary
P27-0	0.27	0	3:1 TFE/DMF	1	stationary
P27-0.5	0.27	0.005	3:1 TFE/DMF	1	stationary
P27-1	0.27	0.010	3:1 TFE/DMF	1	rotating
P27-1.5	0.27	0.015	3:1 TFE/DMF	1	rotating

2. EXPERIMENTAL METHODS

2.1. Materials. SBMA, azobisisobutyronitrile (AIBN), 4-methoxy phenol (MEHQ), bovine serum albumin (BSA, 66.5 kDa), phosphate-buffered saline (PBS), and LiCl were all purchased from Sigma-Aldrich (St. Louis, MO). TFEMA was purchased from Scientific Polymer Products Inc. (Ontario, NY). Trifluoroethanol (TFE), basic activated alumina, dimethyl sulfoxide (DMSO), dimethyl acetamide (DMAc), and dimethyl formamide (DMF) were purchased from VWR (West Chester, PA). Deuterated DMSO (DMSO-d_6) and deuterium oxide (D_2O) were obtained from Cambridge Isotope Laboratory (Tewksbury, MA). All chemicals and solvents were of reagent grade and used as received, except TFEMA, which was purified by passing through a basic activated alumina column.

2.2. Synthesis and Characterization of PTFEMA-*r*-SBMA Copolymer. The random copolymer PTFEMA-*r*-SBMA was synthesized by free radical copolymerization using a previously described method[39] with minor modifications. Briefly, TFEMA (Aldrich) was passed through a column of basic activated alumina to remove the inhibitor. Then, 0.1 g of LiCl was dissolved in 100 mL of DMSO in a round-bottom flask while stirring at 350 rpm. Two grams of SBMA was added and dissolved. TFEMA (8 g) and AIBN (0.0125 g) were added to the round-bottom flask to achieve a TFEMA/SBMA ratio of 80:20 by mass. The flask was sealed with a rubber septum. Nitrogen was bubbled through the reaction mixture for 20 min to purge any dissolved oxygen. The flask was then kept in an oil bath set to 70 °C while stirring at 350 rpm for at least 48 h. After the reaction, 0.5 g of MEHQ was added to terminate the reaction. The copolymer was precipitated in water, collected, and further purified by washing in a 1:1 ethanol/hexane mixture by volume overnight twice. The copolymer was then dried in the vacuum oven set to 50 °C overnight. The composition of the copolymer, collected as a white powder, was characterized by a proton nuclear magnetic resonance (^{1}H NMR) Bruker Avance III 500 spectrometer using DMSO-d_6 as the solvent.

2.3. Molecular Weight Characterization. Dynamic light scattering (DLS) measurements were conducted using a Nano Brook 90Plus PALS particle sizer (Brookhaven Instruments, Holtsville, NY). The light source of the instrument was a He−Ne laser with a nominal wavelength of 659 nm and 1 mm entrance aperture. The measurements were performed on a 1 mg/mL copolymer solution in DMSO at a scattering angle of 90° and a temperature of 25 °C. Before any measurement, the copolymer solution was passed through a 0.2 μm Teflon filter to remove impurities. Then, five consecutive measurements were performed following a stabilization period of 2 min. The effective hydrodynamic radius value was used to calculate the relative molecular weight based on PMMA standards in tetrahydrofuran (THF) by implementing the Mark−Houwink equation using the literature values for Mark−Houwink parameters for PMMA in THF at 25 °C, which were $K = 1.28 \times 10^{-2}$ and $a = 0.69$.[54]

2.4. Electrospinning of PTFEMA-*r*-SBMA. Homogenous solutions of PTFEMA-*r*-SBMA were prepared in DMAc, TFE, and DMF/TFE mixtures by stirring overnight at room temperature to obtain a clear polymer solution. If the solution contained LiCl, the salt was fully dissolved in the solvent before the addition of the copolymer. Compositions of polymer solutions used in this study and the codes used to signify them throughout the document are listed in Table 1.

A glass syringe, with an inner diameter of 14.4 mm and a 16 gauge stainless steel needle, was filled with the clear copolymer solution and gently placed horizontally in the syringe pump (Braintree Scientific, Inc. BS-8000) operated to achieve a solution flow rate of 0.005 mL/h. The syringe tip was kept at a working distance of 18 cm from a grounded collector covered by an aluminum foil. Most electrospun mats were collected on a stationary collector. In the few cases where it was difficult to collect uniform mats, a rotary collector was used to acquire the aligned nanofibers. The rotating speed was kept at 500 rpm. A voltage of 22.8 kV was applied to the system with a high voltage power supply (Gamma High Voltage Research Inc. model no. ES30P-5w) during electrospinning. The collected nanofiber mats were placed in a vacuum oven to remove any residual solvent and stored in a desiccator.

2.5. Scanning Electron Microscopy (SEM). SEM images were obtained using a Phenom G2 pure tabletop scanning electron microscope operated at 5 kV. Field emission SEM (Quanta 400 FEG, FEI) was used to show the fiber morphology at high magnifications. Prior to imaging, electrospun nanofiber mat samples were fixed onto a sample holder with a double-sided carbon conductive tape and were sputter coated with the gold/palladium (60/40) alloy for 120 s at 30 mA current in an argon atmosphere. Average fiber diameter (AFD) was calculated using ImageJ by analyzing more than 100 fibers from 3 images acquired for each sample.

2.6. Rheometry. At least 3 mL of each polymer solution was prepared by stirring for at least 3 h. All solutions were prepared on the day of the analysis. These solutions were tested using a TA Instruments ARES-LS2 shear rheometer (New Castle, DE) with a cone and plate assembly 50 mm in diameter and with a cone angle of 0.0402 rad. Samples were allowed to equilibrate for 30 s at each shear rate prior to averaging the viscosity over 10 s.

2.7. X-ray Photoelectron Spectroscopy (XPS). PHI-5000 VersaProbe spectrometer equipped with a monochromatic Al Kα radiation source (1486.6 eV) was used for XPS analysis. Fiber mats were allowed to vacuum dry overnight prior to the day of analysis. A piece of fiber mat was placed on the sample holder and moved into the analysis chamber. A survey scan was conducted to determine the elemental composition of the fiber surface. High-resolution scans were conducted for all elements in the polymer structure, though the data analysis in this paper focuses on the C 1s region.

2.8. CA Measurements. The surface hydrophobicity of the electrospun fiber mats was evaluated by conducting sessile drop CA measurements. A ramé-hart CA instrument (Succasunna, NJ) equipped with a horizontal microscope and camera connected to a video screen was used for imaging, and DROPimage Advanced version 2.4.05 software was used for the analysis. For the measurements, the electrospun mats were mounted on a glass slide using a double-sided tape, and then, a 2 μL droplet of deionized water was dispensed onto each mat. The internal angles of both sides of the water droplet were determined for three droplets at three different locations per sample.

DOI: 10.1021/acsami.8b03268
ACS Appl. Mater. Interfaces XXXX, XXX, XXX−XXX

The mean value ± standard deviation calculated from three different samples is reported.

2.9. X-ray Diffraction (XRD) Analysis. One-dimensional XRD was performed in the reflection mode at room temperature using a Philips PW 1830 powder diffractometer. The generator produced X-rays of wavelength λ = 0.1542 nm (Cu Kα radiation) and was operated at 40 kV and 45 mA. Samples were examined in the θ–2θ reflection mode (for θ the half scattering angle) using a step scan interval of 0.02°/step and a scanning rate of 0.01°/s from 2θ = 5–35°. A piece of electrospun mat was cut and attached to a rectangular sample holder and placed into the XRD instrument.

2.10. Attenuated Total Reflection Fourier Transform Infrared (ATR–FTIR) Spectroscopy. The ATR-FTIR spectra of the as-spun nanofibers were recorded using a JASCO FT/IR-6200 spectrometer (JASCO Instruments, Easton, MD). The measurements were conducted on lyophilized PTFEMA-*r*-SBMA nanofibers prepared with or without LiCl. Samples were placed on the ATR crystal and held in place by a clamp. The data were collected in air. Spectra were scanned in the absorption mode at 4 cm^{-1} resolution from 4000 to 400 cm^{-1}. One hundred and twenty-eight scans were taken for each sample to improve the signal to noise ratio. Spectra were analyzed using OPUS software (version 5.0) (Mattson Instruments, Madison, WA).

2.11. Protein Adsorption and Fouling Measurements. The electrospun fiber mats were tested for their protein fouling resistance, following a procedure adopted from J. Seo and J.-H. Seo.[51] Fluorescein isothiocyanate-labeled BSA (5 mg/L) in PBS was used as the foulant solution. Sections of dimensions 5 cm × 5 cm were cut out from the electrospun fiber mats and then fully immersed in the foulant solution for 10 min on a nutating mixer. Once the mats were taken out of the foulant solution, they were washed three times by dipping into fresh PBS solution. The mats were then imaged under an epifluorescence microscope (Olympus BX51 equipped with a DP70 microscope digital camera, Center Valley, PA). A 20× objective lens with a standard green (U-N31001) filter set (Chroma Technology Corp., Rockingham, VT) was implemented for obtaining the epifluorescence micrographs. ImageJ image analysis software was used to measure the fluorescence intensity from five different 100 μm × 100 μm sections of each image, and then, these intensity values were used to calculate the average fluorescence intensity for each image.

3. RESULTS AND DISCUSSION

3.1. PTFEMA-*r*-SBMA Copolymer Synthesis and Characterization. In this study, electrospun fibers and mats were prepared from a random copolymer of a fluorinated monomer, TFEMA, and a zwitterionic monomer, SBMA. This copolymer, PTFEMA-*r*-SBMA, was previously found to be extremely fouling-resistant when used as a membrane selective layer.[39−41] However, the copolymers used in all these studies had a high SBMA content (≳30 wt %) to enable water permeability.[39] These copolymers are highly plasticized with water and become hydrophilic upon immersion into water, as the zwitterionic functional groups segregate on the surface.[40] To create hydrophobic electrospun materials that include zwitterionic groups, we prepared PTFEMA-*r*-SBMA by free radical copolymerization (Figure 1), following a previously reported protocol.[6] The starting monomer mixture contained 20 wt % SBMA. The resultant copolymer contained 20 wt % SBMA at a conversion of 70%, as documented by ^{1}H NMR spectroscopy (Supporting Information, Figure S1). Previous work[39,40] predicts that if used as a membrane selective layer, this copolymer would be essentially impermeable to water. Therefore, we have not previously characterized the fouling resistance or surface properties of copolymers with such a low SBMA content. On the other hand, when formed into fibers, we would expect these copolymers to be highly stable upon exposure to water, creating the structural components of porous mats and membranes formed by electrospinning.

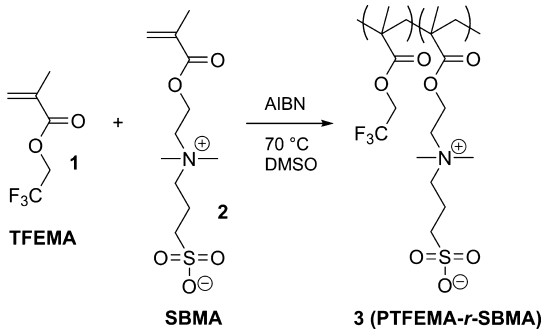

Figure 1. Synthesis scheme for the PTFEMA-*r*-SBMA copolymer by free radical copolymerization.

To obtain an estimate of the molecular weight of the PTFEMA-*r*-SBMA copolymer, DLS was used to measure the hydrodynamic radius. DLS was performed on a 1 mg/mL solution of the copolymer in DMSO. The effective hydrodynamic radius was found to be 62 ± 13 nm. The relative molar mass was calculated to be 6.6 × 10^5 g/mol using Mark–Houwink constants for PMMA standards in THF at 25 °C. It should be noted that this value is an order-of-magnitude estimate rather than an absolute molecular weight because of the variable polymeric chain conformations based on solvent–polymer interactions.

3.2. Effect of the Electrospinning Solvent. A critical parameter in the optimization of an electrospinning system is the choice of the solvent in which the polymer is dissolved. The viscosity, solvent quality, polarity, surface tension, and volatility of the solvent all influence the resultant electrospun structure.[55] This choice is relatively limited for the electrospinning of the PTFEMA-*r*-SBMA copolymer because its two types of repeat units are very different in nature and have few common solvents. This, combined with the strong Coulombic interactions between the charged groups on the zwitterions, leads to few available solvents for this copolymer. The copolymer was found to be easily soluble in TFE. It was also soluble in DMAc. Although it was not sufficiently soluble in DMF at the concentrations needed for electrospinning, the addition of TFE into this solvent enabled it to dissolve. To identify the best electrospinning solvent system, three PTFEMA-*r*-SBMA solutions were prepared, each containing 0.18 g of the copolymer mixed with 1 mL of a different solvent or solvent mixture (Table 1). The solution in DMAc, P-DMAc, did not produce electrospun mats and only led to electrospraying of small droplets despite multiple conditions tested (Figure 2, left), possibly due to the low volatility and high

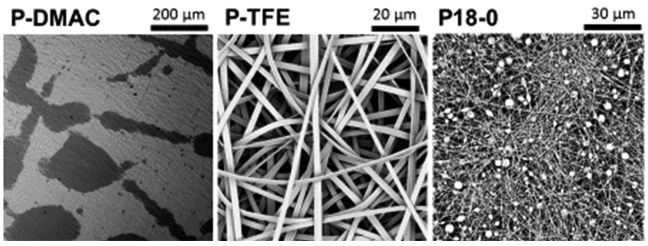

Figure 2. SEM images of electrospun mats prepared using different solvents. P-DMAC was prepared from DMAc, P-TFE was prepared from TFE, and P18-0 was prepared from a 3:1 DMF/TFE.

DOI: 10.1021/acsami.8b03268
ACS Appl. Mater. Interfaces XXXX, XXX, XXX−XXX

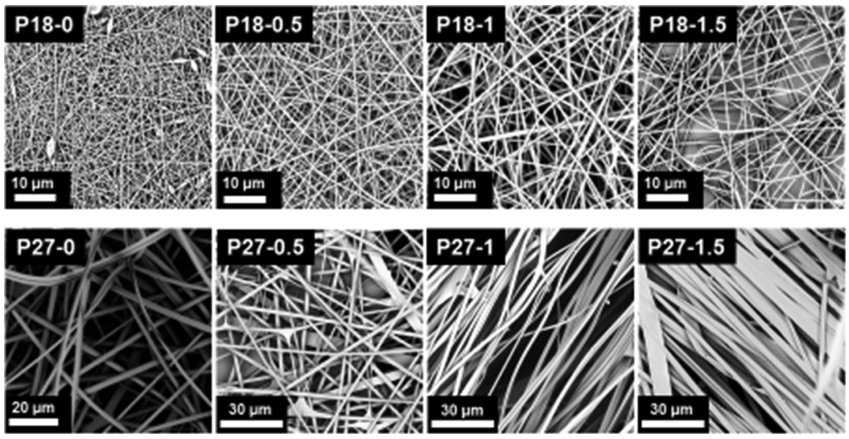

Figure 3. SEM images of electrospun mats prepared from solutions containing various copolymer and LiCl concentrations, demonstrating a wide range of accessible morphologies including beaded and bead-free nanofibers, microfibers, and ribbonlike fibers.

surface tension of this solvent. A different solvent system that has a lower surface tension may enable the Coulombic forces created by the applied voltage to overcome the surface tension of the solution, so that fibers can be formed on the collector.

Electrospun mats prepared from TFE led to the creation of ribbonlike fibers, ~2600 ± 300 nm in width and 530 ± 80 nm in thickness (Figure 2, middle). Ribbonlike morphologies are believed to arise from the formation of a skin on the liquid jet because of the rapid evaporation of the solvent, followed by the collapse of this skin.[33,56] The high volatility of this solvent, however, also often caused the needle to clog during the electrospinning process, resulting in fiber breakage.

Finally, fibers electrospun from 3:1 mixtures of DMF with TFE led to beaded nanofibers (Figure 2, right). Despite the presence of beads, considered undesirable for most electrospun materials,[33] this solvent composition was selected because of better, more reliable processing and the potential for tuning the fiber morphology through the use of other parameters such as copolymer composition and the addition of salts.

3.3. Effect of Copolymer Concentration on the Morphology. The copolymer concentration in the electrospinning solution directly affects the solution viscosity, surface tension, and the rate at which the polymer is dispensed by the syringe pump. As such, copolymer concentration is one of the most important parameters in controlling and tuning the morphology of resultant electrospun fibers and mats. In this study, electrospun mats were prepared from 18 or 27 g copolymer per 100 mL of the solvent mixture, without any added LiCl, denoted as P18-0 and P27-0, respectively (Table 1). Electrospinning of the more dilute P18-0 created beaded nanofibers (Figure 3), ~200 nm in diameter (Table 2). Increasing the copolymer concentration is a common approach to achieve bead-free electrospun fibers.[33] Indeed, bead-free fibers were obtained from P27-0. The fiber diameter also increased significantly to micron scale (Figure 3, Table 2), in agreement with other studies showing that increased polymer concentration often leads to a larger fiber diameter.[57] A small number of flat or dumbbell-shaped fibers can also be observed upon careful inspection. Higher magnification images (see Supporting Information, Figure S2) show that many of the cylindrical fibers have wrinkled surfaces. These fiber morphologies likely arise from the fast evaporation of TFE from the surface of the fibers, creating a thin skin layer. As the rest of the solvent is removed, this skin layer collapses.[56,58] This is known as the buckling instability. Buckling can also occur if a thin, gelled, or glassy surface film forms due to phase separation instead of evaporation. This can occur, for example, because of the water vapor present in humid air acting as a nonsolvent for the polymer.[59] The occurrence of buckling before the complete removal of the solvent from the fiber core leads to noncircular fiber cross-sections such as flat or dumbbell-shaped fibers or wrinkly fibers with a high surface area.[56,58,59]

Table 2. AFD and Standard Deviations for Electrospun Mats

sample name	AFD (nm)
P18-0	230 ± 27
P18-0.5	202 ± 23
P18-1	415 ± 48
P18-1.5	503 ± 61
P27-0	2230 ± 390
P27-0.5	2200 ± 360
P27-1	2350 ± 310
P27-1.5	3140 ± 520

3.4. Effect of LiCl Addition to Electrospinning Solution. The addition of salts to electrospinning solutions increases the net charge density, leading to increased electrostatic repulsions on the fiber surface and the spinning of more bead-free fibers.[33] However, salt addition to a polymer solution also changes the solution viscosity and surface tension, which in turn affects the electrospun fiber morphology. Of these parameters, the increase in the solution charge density and conductivity typically leads to thinner fibers. In addition to charge effects, salt addition can also change the solvent quality for the dissolved copolymer. This would in turn change the swelling and conformation of the polymer chains in solution, which would affect the flow properties and spinnability of the solution and the chain conformation in the fibers. These two competing effects have been widely studied for the control and modulation of the electrospun fiber morphology.[60,61]

Zwitterionic polymers are subject to significant changes in the solvency and intra- and intermolecular interactions in response to the presence of small ions. In the absence of small ions, strong Coulombic interactions between the anionic and cationic groups on each zwitterionic group (e.g., the sulfonate and quaternary amine groups forming the sulfobetaine moiety in SBMA) lead to the formation of intrachain associations that limit the solubility and result in collapsed polymer chains. Upon

DOI: 10.1021/acsami.8b03268
ACS Appl. Mater. Interfaces XXXX, XXX, XXX−XXX

the addition of small ions (i.e., a salt such as LiCl or NaCl), these intrachain associations are broken, as Coulombic interactions are partially shielded by the salt ions. Solvency increases and polymer chains swell.[44,62] Interchain associations between zwitterionic groups can also be present with or without these small ions. These interactions act as physical cross-links between chains.[63,64] This effect, termed the anti-polyelectrolyte effect, has been extensively studied in aqueous systems.[44,62,63,65,66] There are few, if any, studies on this phenomenon in organic solvents such as those used for electrospinning in this study or on its effect on electrospinning. However, given the literature indicating the importance of zwitterion−zwitterion interactions on electrospinning,[48] the addition of a salt to these polymer solutions may be a crucial tool for controlling the morphology of electrospun fibers.

Indeed, our previous exploratory studies with PTFEMA-*r*-SBMA and other zwitterion-containing random copolymers had indicated that the addition of LiCl to organic solvents like DMSO increased their solubility in these organic solvents.[6,39,40] This implies that the addition of LiCl salt to concentrated PTFEMA-*r*-SBMA solutions would change many parameters simultaneously including, but not limited to, solution conductivity, inter-molecular interactions between zwitterionic groups, solvent quality for the zwitterionic segments, and solvent quality for the hydrophobic polymer segments. These two factors would be reflected in the flow properties of the copolymer solutions.

To better understand how salt addition affects the flow properties of concentrated PTFEMA-*r*-SBMA solutions in the DMF/TFE mixtures including some used for electrospinning, rheometry was performed on a range of polymer solutions containing 27 g of copolymer and 0−1.5 g of LiCl per 100 mL of the solvent, labeled P27-0 to P27-1.5 (Table 1). The viscosities of the copolymer solutions were measured at varying shear rates to better characterize their viscoelastic properties. The P27-0 solution, with no LiCl added, had a viscosity around 4.1 P at low shear rates (Figure 4). Although the solution viscosity decreased slightly to ∼3.6 P at high shear rates, the shear thinning effect was minor and entirely typical for polymer solutions. This was also similar to the results reported for concentrated solutions of the zwitterionic random copolymers PBMA-*r*-SBMA[48] and PMMA-*r*-CBMA[50] and the PSBMA homopolymer[45] in the absence of the salt. By contrast, upon the addition of even small amounts of LiCl, the solution viscosity increased greatly at low shear rates to around 100 P, with higher salt concentrations leading to slightly higher viscosities. The solutions also exhibited significant shear thinning, with viscosity decreasing by over an order of magnitude with increasing shear rate. These results imply that the copolymer chains are in a relatively collapsed form in the absence of a salt, with isolated coils in solution. When LiCl is added to the solution, the chains expand, leading to increased viscosity. This effect, termed as the anti-polyelectrolyte effect, has been extensively reported for polyzwitterions in aqueous solution.[44,45,63] These results indicate that a similar outcome is observed in this organic solvent. Upon chain swelling, transient interactions between zwitterionic groups on different polymer chains likely act in a manner similar to entanglements, leading to the shear-thinning effect.

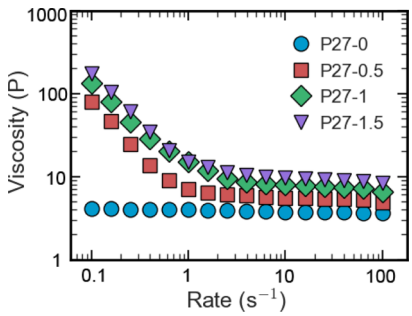

Figure 4. Rheometry results for electrospinning solutions containing 27 g of copolymer and 0−1.5 g of LiCl per 100 mL of the solvent. The solutions show roughly Newtonian behavior in the absence of LiCl, as shown in P27-0. Viscosity increases significantly upon the addition of LiCl, and the solutions become shear-thinning.

There were important morphological differences between electrospun mats and fibers prepared from solutions containing LiCl (Figure 3). The addition of even small amounts of LiCl to the lower polymer concentrations (P18 series) enabled the electrospinning of bead-free fibers. This is in agreement with the results for other polymer systems, where the increased solution conductivity improves fiber stretching during the electrospinning process and prevents bead formation.[67,68] Further addition of LiCl to the polymer solution led to an increase in the fiber diameter (Table 2).

When a higher polymer concentration was used (P27 series), bead-free fibers were obtained in the absence of any salts. LiCl addition led to a transition from fibers with circular cross-sections to flat, ribbonlike fibers. This was observed both in P27-0.5, where a stationary collector was used, and in P27-1 and P27-1.5, collected on a rotating drum to improve the uniformity of the deposited mat. This may have arisen from the fact that a mixture of two solvents, highly volatile TFE and less volatile DMF, was used in this process. The fast evaporation of TFE in these systems likely leads to the formation of a thin skin layer. The fiber then collapses as the DMF evaporates, creating flat fibers.[56] At high polymer and salt concentrations, the polymer is closer to the gel point. The skin layer forms quickly upon the removal of even a small amount of TFE from the system, creating a ribbonlike morphology. This resulted in an increase in the average diameter of the fibers calculated by image analysis with increasing LiCl concentration (Table 2), as the ribbons became more common and wider.

To better characterize the chain arrangement within the fibers, XRD was performed on the P27-0 series fibers (Figure S3). The PTFEMA-*r*-SBMA polymer was synthesized by free radical polymerization and is hence expected to be atactic. Therefore, no crystallinity was expected in the polymer. This was consistent with the XRD data for P27-0 fibers, which showed only a broad amorphous peak at a 2θ of 18°, indicating an average interatom spacing of 0.49 nm, independent of the LiCl content. Interestingly, despite the large LiCl content in the fibers, there were no visible peaks arising from LiCl crystals. The copolymer prevented the crystallization of LiCl during fiber formation, further indicating the strong interaction between zwitterionic groups in the copolymer with salt ions.

3.5. LiCl Addition and Surface Chemistry of Electrospun Fibers. The interaction between salt ions and zwitterionic groups can lead to changes in how the polymer chains are arranged in the fibers and which groups segregate on the fiber surface. This would in turn affect both the hydrophobicity and fouling resistance. To study the effect of LiCl addition on the presence of hydrophobic and hydrophilic groups on the fiber surfaces, we used XPS to characterize the

DOI: 10.1021/acsami.8b03268
ACS Appl. Mater. Interfaces XXXX, XXX, XXX−XXX

surface chemistry of the electrospun mats. We specifically focused on the P18 series, which lead to the formation of unaligned fiber mats at every LiCl concentration. The P18 series also had a smaller fiber size, which is in turn linked to smaller pore size and higher break-through pressures crucial for membrane applications. XPS survey scans confirmed increasing amounts of LiCl in the fibers spun from solutions with a greater LiCl content, as expected (Table 3). Interestingly, as the LiCl concentration in the spinning solution increased, the oxygen content on the fiber surface also increased whereas the fluorine content decreased (Figure 5A).

Table 3. Surface Elemental Composition (at. %) of P18-Series Electrospun Fibers Obtained from XPS Survey Scans

	P18-0	P18-0.5	P18-1	P18-1.5
C 1s	52.8	52.6	53.3	53.5
F 1s	27.8	26.6	25.3	24.7
O 1s	17.2	17.55	18.7	19
N 1s	1.4	1.5	1.1	0.7
S 2p	0.8	1.11	0.7	0.8
Cl 2p	0	0.64	0.9	1.2

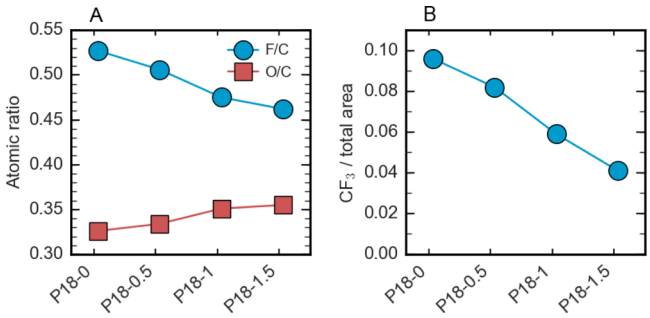

Figure 5. XPS analysis of the effect of LiCl concentration in spinning solution on the fiber surface chemistry. (A) F/C and O/C atomic ratios obtained from XPS survey scans, indicating an enrichment of oxygen atoms and depletion of fluorine atoms on the fiber surface with increasing LiCl addition. (B) The ratio of the peak area for CF_3 groups to the total C 1s peak area obtained from the high-resolution scans, indicating a decrease in the prevalence of fluorinated groups on the fiber surface.

This observation obtained from the survey scan was confirmed using C 1s high-resolution scans (Figure 6), which were analyzed to identify specific functional groups on the fiber surface. The peak at 248.8 eV was assigned to C−C/C−H groups, whereas the peaks at around 286 and 289 eV were assigned to C−O/S/N and COO groups, respectively. CF_3 functional groups from TFEMA units led to the highest binding energy peak, around 293 eV.[69,70] A stronger CF_3 peak was observed in samples prepared with low or no LiCl added to the solution. The area of the CF_3 peak relative to the total peak area decreased with increasing LiCl concentration in the electrospinning solution (Figure 5b). This indicated that CF_3 groups in the TFEMA units in the copolymer were less likely to be on the surface when LiCl was used.

3.6. Hydrophobicity and Fouling Resistance. Finally, we aimed to quantify the hydrophobicity and fouling resistance of electrospun membranes prepared from PTFEMA-*r*-SBMA. These experiments were exclusively performed on samples prepared without any LiCl addition, to avoid complications arising from the leaching of LiCl upon contact with water.

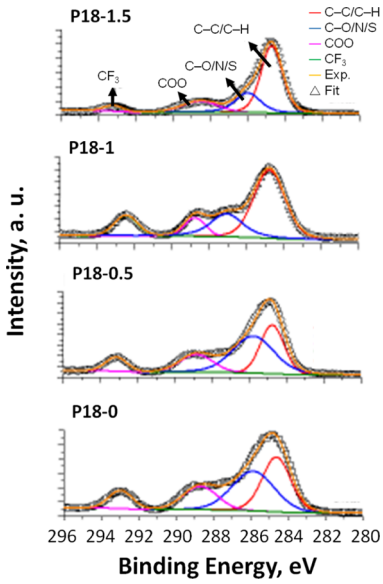

Figure 6. High-resolution C 1s XPS spectra for the P18-series samples.

The CAs of both P18-0 and P27-0 membranes were very high, around 140°, indicating a highly hydrophobic surface (Table 4). These CAs are promising for MD applications.

Table 4. CA of Electrospun Mats before and after Fouling

sample	CA (deg)	CA after fouling (deg)
PVDF (control)	144 ± 2	79 ± 4
P18-0	141 ± 4	132 ± 3
P27-0	136 ± 5	129 ± 6

There are, however, other commodity polymers that can be electrospun to create similarly hydrophobic porous materials. As a control, we prepared an electrospun mat from PVDF, a common material for membranes used in filtration and MD applications.[6,12] This PVDF mat had a morphology and fiber size similar to that of the P18-0 membrane (see the Supporting Information, Figure S4) and a comparable, though slightly higher, initial CA of 144°.

To test the effect of exposure to organic foulants on the surface hydrophobicity of these materials, we dipped each mat in a protein solution containing 1 g/L BSA in PBS. This solution is commonly used to test the fouling resistance of membrane materials because BSA is a protein that easily and strongly adsorbs on a wide variety of surfaces.[1,4,15,16] Upon adsorption, the protein covers the surfaces and makes them relatively more hydrophilic. In MD, this can allow the feed to break through the porous membrane, contaminating the permeate, increasing its temperature, and decreasing the efficiency and effluent quality of the operation.[16] In our tests, we found that after exposure to the protein solution, the CA of the PVDF mat decreased drastically to only 79° (Table 3). This CA is below 90° and indicates that the material wets easily. By contrast, the two zwitterion-containing membranes remained highly hydrophobic, with CAs remaining around 130°. This implies that these membranes would operate reliably even with feeds that contain biomacromolecular contaminants with a high fouling potential.

DOI: 10.1021/acsami.8b03268
ACS Appl. Mater. Interfaces XXXX, XXX, XXX−XXX

To further document the fouling resistance of these materials, we performed a quantitative protein adsorption experiment. A 5 cm × 5 cm swatch was cut out from the P18-0 and PVDF mats. Both of these mats were immersed into a 5 mg/L solution of fluorescently labeled BSA for 10 min on a nutating mixer, rinsed, and then imaged using an epifluorescence microscope. The mean fluorescence intensity measured for each sample is directly proportional to the amount of fluorescently labeled protein adsorbed onto the mat, and hence a measure of propensity for protein fouling. The electrospun PTFEMA-*r*-SBMA mat, P18-0, adsorbed approximately 80% less protein than the PVDF mat (Figure 7). This result was confirmed with a separate, simple, qualitative experiment. One half of each mat, P18-0 and control PVDF, was immersed in a 1 g/L BSA solution in PBS for 18 h and then rinsed. The protein was stained with the GelCode Blue Safe Protein Stain. Foulant-dipped parts of the PVDF mat showed large patches of protein deposits. By contrast, the P18-0 mat showed no visible blue staining, indicating little if any protein adsorption (Supporting Information, Figure S5). These tests synergistically confirm the ability of this zwitterionic copolymer to maintain hydrophobicity while resisting fouling.

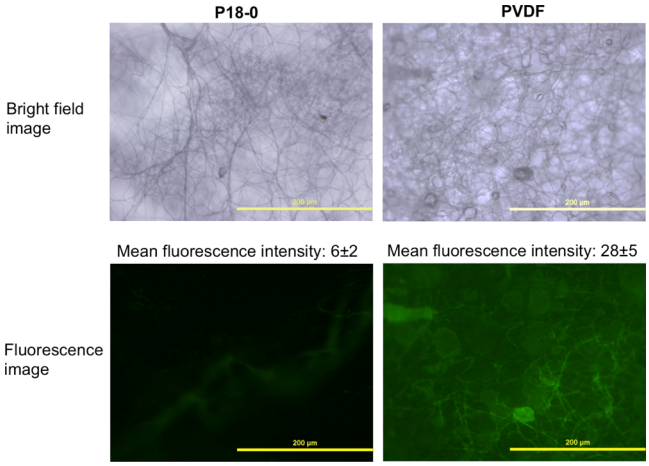

Figure 7. Bright-field (top row) and fluorescence (bottom row) images of the mats obtained after exposure to fluorescently labeled BSA adsorption. In the fluorescence images (bottom row), green color intensifies with increasing fluoresced foulant protein adsorbed on the membrane. P18-0 mat shows approximately 80% less protein adsorption than the PVDF mat. The scale bars are 200 μm.

4. CONCLUSIONS

This study is the first report of the formation of electrospun membranes from PTFEMA-*r*-SBMA, a copolymer of zwitterionic and fluorinated monomers. A wide range of fiber morphologies (beaded fibers, bead-free fibers, ribbon-like fibers, and wrinkly fibers) can be obtained by altering the solvent composition, by changing the copolymer concentration, and by adding LiCl to the spinning solution. The resultant electrospun membranes are highly hydrophobic, yet adsorb 80% less protein in comparison with a PVDF membrane with a similar initial CA. Their CA also remains stable even after exposure to a protein solution, further confirming their fouling resistance. These highly hydrophobic yet fouling-resistant membranes are promising for several applications, especially MD. Our findings are also relevant to the preparation of a wide range of fouling-resistant porous materials by electrospinning.

■ ASSOCIATED CONTENT

Supporting Information

The Supporting Information is available free of charge on the ACS Publications website at DOI: 10.1021/acsami.8b03268.

^{1}H NMR spectrum of the copolymer, high-resolution SEM image of the P27-0 fiber, SEM images of P18-0 and PVDF mats, and image of fouled mats upon protein staining (PDF)

■ AUTHOR INFORMATION

Corresponding Author

*E-mail: ayse.asatekin@tufts.edu.

ORCID

Ayse Asatekin: 0000-0002-4704-1542

Author Contributions

The manuscript was written through contributions of all authors. All authors have given approval to the final version of the manuscript.

Funding

This research was funded by the Tufts University, the Tufts Collaborates Program, and the National Science Foundation (NSF) under grant nos. CBET-1437772, CHE-1508049, and DMR1608125.

Notes

The authors declare no competing financial interest.

■ ACKNOWLEDGMENTS

The authors thank David Wilbur for help with the NMR analysis, Methira Saksiriwatekul for experimental help with SEM and DLS measurements, and Prof. Qiaobing Xu for access to DLS equipment. The authors also thank Prof. Hyunmin Yi and Eric Liu for access to the Epifluorescence Microscopy facility and help with experimental training and design. This research was funded by the Tufts University and the National Science Foundation (NSF) under grant nos. CBET-1437772, CHE-1508049, and DMR-1608125.

■ ABBREVIATIONS

MD, membrane distillation; AIBN, azobisisobutyronitrile; MEHQ, 4-methoxy phenol; TFE, trifluoroethanol; PTFEMA-*r*-SBMA, poly(trifluoroethyl methacrylate-*random*-sulfobetaine methacrylate); PVDF, polyvinylidene fluoride; DMSO, dimethyl sulfoxide; NMR, nuclear magnetic resonance; M_w, molecular weight; DLS, dynamic light scattering; PAN, polyacrylonitrile; DMF, dimethyl formamide; DMAc, dimethylacetamide; SEM, scanning electron microscopy; XPS, X-ray photoelectron spectroscopy; CA, contact angle; XRD, X-ray diffraction; ATR−FTIR, attenuated total reflection Fourier transform; BSA, bovine serum albumin; FITC, fluorescein isothiocyanate; PBS, phosphate buffered saline

■ REFERENCES

(1) Yang, R.; Asatekin, A.; Gleason, K. K. Design of conformal, substrate-independent surface modification for controlled protein adsorption by chemical vapor deposition (CVD). *Soft Matter* **2012**, *8*, 31−43.

(2) Holmlin, R. E.; Chen, X.; Chapman, R. G.; Takayama, S.; Whitesides, G. M. Zwitterionic SAMs that resist nonspecific adsorption of protein from aqueous buffer. *Langmuir* **2001**, *17*, 2841−2850.

(3) Ostuni, E.; Chapman, R. G.; Holmlin, R. E.; Takayama, S.; Whitesides, G. M. A survey of structure-property relationships of

DOI: 10.1021/acsami.8b03268
ACS Appl. Mater. Interfaces XXXX, XXX, XXX−XXX

surfaces that resist the adsorption of protein. *Langmuir* **2001**, *17*, 5605−5620.

(4) Banerjee, I.; Pangule, R. C.; Kane, R. S. Antifouling Coatings: Recent Developments in the Design of Surfaces That Prevent Fouling by Proteins, Bacteria, and Marine Organisms. *Adv. Mater.* **2011**, *23*, 690−718.

(5) Kaner, P.; Johnson, D. J.; Seker, E.; Hilal, N.; Altinkaya, S. A. Layer-by-layer surface modification of polyethersulfone membranes using polyelectrolytes and AgCl/TiO2 xerogels. *J. Membr. Sci.* **2015**, *493*, 807−819.

(6) Kaner, P.; Rubakh, E.; Kim, D. H.; Asatekin, A. Zwitterion-containing polymer additives for fouling resistant ultrafiltration membranes. *J. Membr. Sci.* **2017**, *533*, 141−159.

(7) Kaner, P.; Hu, X.; Thomas, S. W.; Asatekin, A. Self-Cleaning Membranes from Comb-Shaped Copolymers with Photoresponsive Side Groups. *ACS Appl. Mater. Interfaces* **2017**, *9*, 13619−13631.

(8) Baxamusa, S. H.; Gleason, K. K. Random Copolymer Films with Molecular-Scale Compositional Heterogeneities that Interfere with Protein Adsorption. *Adv. Funct. Mater.* **2009**, *19*, 3489−3496.

(9) Gudipati, C. S.; Finlay, J. A.; Callow, J. A.; Callow, M. E.; Wooley, K. L. The antifouling and fouling-release perfomance of hyper-branched fluoropolymer (HBFP)-poly(ethylene glycol) (PEG) composite coatings evaluated by adsorption of biomacromolecules and the green fouling alga Ulva. *Langmuir* **2005**, *21*, 3044−3053.

(10) Weinman, C. J.; Gunari, N.; Krishnan, S.; Dong, R.; Paik, M. Y.; Sohn, K. E.; Walker, G. C.; Kramer, E. J.; Fischer, D. A.; Ober, C. K. Protein adsorption resistance of anti-biofouling block copolymers containing amphiphilic side chains. *Soft Matter* **2010**, *6*, 3237−3243.

(11) Youngblood, J. P.; Andruzzi, L.; Ober, C. K.; Hexemer, A.; Kramer, E. J.; Callow, J. A.; Finlay, J. A.; Callow, M. E. Coatings based on side-chain ether-linked poly(ethylene glycol) and fluorocarbon polymers for the control of marine biofouling. *Biofouling* **2003**, *19*, 91−98.

(12) Eykens, L.; De Sitter, K.; Dotremont, C.; Pinoy, L.; Van der Bruggen, B. Membrane synthesis for membrane distillation: A review. *Sep. Purif. Technol.* **2017**, *182*, 36−51.

(13) Thomas, N.; Mavukkandy, M. O.; Loutatidou, S.; Arafat, H. A. Membrane distillation research & implementation: Lessons from the past five decades. *Sep. Purif. Technol.* **2017**, *189*, 108−127.

(14) Tijing, L. D.; Woo, Y. C.; Choi, J.-S.; Lee, S.; Kim, S.-H.; Shon, H. K. Fouling and its control in membrane distillation—A review. *J. Membr. Sci.* **2015**, *475*, 215−244.

(15) Baker, J. S.; Dudley, L. Y. Biofouling in membrane systems—a review. *Desalination* **1998**, *118*, 81−89.

(16) Laqbaqbi, M.; Sanmartino, J.; Khayet, M.; García-Payo, C.; Chaouch, M. Fouling in Membrane Distillation, Osmotic Distillation and Osmotic Membrane Distillation. *Appl. Sci.* **2017**, *7*, 334.

(17) Kayaci, F.; Vempati, S.; Ozgit-Akgun, C.; Donmez, I.; Biyikli, N.; Uyar, T. Transformation of polymer-ZnO core−shell nanofibers into ZnO hollow nanofibers: Intrinsic defect reorganization in ZnO and its influence on the photocatalysis. *Appl. Catal., B* **2015**, *176−177*, 646−653.

(18) Aytac, Z.; Sen, H. S.; Durgun, E.; Uyar, T. Sulfisoxazole/cyclodextrin inclusion complex incorporated in electrospun hydroxypropyl cellulose nanofibers as drug delivery system. *Colloids Surf., B* **2015**, *128*, 331−338.

(19) Zhu, Y.; Pyda, M.; Cebe, P. Electrospun fibers of poly(l-lactic acid) containing lovastatin with potential applications in drug delivery. *J. Appl. Polym. Sci.* **2017**, *134*, 45287.

(20) Zhu, Y.; Li, C.; Cebe, P. Poly(lactides) co-electrospun with carbon nanotubes: thermal and cell culture properties. *Eur. Polym. J.* **2016**, *75*, 565−576.

(21) Bradner, S. A.; Partlow, B. P.; Cebe, P.; Omenetto, F. G.; Kaplan, D. L. Fabrication of elastomeric silk fibers. *Biopolymers* **2017**, *107*, No. e23030.

(22) Bui, N.-N.; Lind, M. L.; Hoek, E. M. V.; McCutcheon, J. R. Electrospun nanofiber supported thin film composite membranes for engineered osmosis. *J. Membr. Sci.* **2011**, *385−386*, 10−19.

(23) Bui, N.-N.; McCutcheon, J. R. Nanoparticle-embedded nanofibers in highly permselective thin-film nanocomposite membranes for forward osmosis. *J. Membr. Sci.* **2016**, *518*, 338−346.

(24) Huang, L.; Arena, J. T.; McCutcheon, J. R. Surface modified PVDF nanofiber supported thin film composite membranes for forward osmosis. *J. Membr. Sci.* **2016**, *499*, 352−360.

(25) Wunderlich, B. Reversible crystallization and the rigid−amorphous phase in semicrystalline macromolecules. *Prog. Polym. Sci.* **2003**, *28*, 383−450.

(26) Pak, J.; Pyda, M.; Wunderlich, B. Rigid Amorphous Fractions and Glass Transitions in Poly(oxy-2,6-dimethyl-1,4-phenylene). *Macromolecules* **2003**, *36*, 495−499.

(27) Suzuki, H.; Grebowicz, J.; Wunderlich, B. Glass transition of poly(oxymethylene). *Br. Polym. J.* **1985**, *17*, 1−3.

(28) Androsch, R.; Wunderlich, B. The link between rigid amorphous fraction and crystal perfection in cold-crystallized poly(ethylene terephthalate). *Polymer* **2005**, *46*, 12556−12566.

(29) Menczel, J.; Wunderlich, B. Heat-Capacity Hysteresis Of Semi-Crystalline Macromolecular Glasses. *J. Polym. Sci., Polym. Lett. Ed.* **1981**, *19*, 261−264.

(30) Ma, Q.; Pyda, M.; Mao, B.; Cebe, P. Relationship between the rigid amorphous phase and mesophase in electrospun fibers. *Polymer* **2013**, *54*, 2544−2554.

(31) Gibson, P.; Schreuder-Gibson, H.; Rivin, D. Transport properties of porous membranes based on electrospun nanofibers. *Colloids Surf., A* **2001**, *187−188*, 469−481.

(32) Greiner, A.; Wendorff, J. H. Electrospinning: A Fascinating Method for the Preparation of Ultrathin Fibers. *Angew. Chem., Int. Ed.* **2007**, *46*, 5670−5703.

(33) Li, D.; Xia, Y. Electrospinning of Nanofibers: Reinventing the Wheel? *Adv. Mater.* **2004**, *16*, 1151−1170.

(34) Zhang, Z.; Chao, T.; Chen, S.; Jiang, S. Superlow fouling sulfobetaine and carboxybetaine polymers on glass slides. *Langmuir* **2006**, *22*, 10072−10077.

(35) Zhang, Z.; Chen, S.; Chang, Y.; Jiang, S. Surface grafted sulfobetaine polymers via atom transfer radical polymerization as superlow fouling coatings. *J. Phys. Chem. B* **2006**, *110*, 10799−10804.

(36) Kitano, H.; Kawasaki, A.; Kawasaki, H.; Morokoshi, S. Resistance of zwitterionic telomers accumulated on metal surfaces against nonspecific adsorption of proteins. *J. Colloid Interface Sci.* **2005**, *282*, 340−348.

(37) Sun, Q.; Su, Y.; Ma, X.; Wang, Y.; Jiang, Z. Improved antifouling property of zwitterionic ultrafiltration membrane composed of acrylonitrile and sulfobetaine copolymer. *J. Membr. Sci.* **2006**, *285*, 299−305.

(38) Kitano, H.; Imai, M.; Gemmei-Ide, M.; Takaha, K. Raman spectroscopic study on the structure of water in aqueous solution of zwitterionic surfactants. *J. Colloid Interface Sci.* **2004**, *269*, 459−465.

(39) Bengani, P.; Kou, Y.; Asatekin, A. Zwitterionic copolymer self-assembly for fouling resistant, high flux membranes with size-based small molecule selectivity. *J. Membr. Sci.* **2015**, *493*, 755−765.

(40) Bengani-Lutz, P.; Converse, E.; Cebe, P.; Asatekin, A. Self-Assembling Zwitterionic Copolymers as Membrane Selective Layers with Excellent Fouling Resistance: Effect of Zwitterion Chemistry. *ACS Appl. Mater. Interfaces* **2017**, *9*, 20859−20872.

(41) Bengani-Lutz, P.; Zaf, R. D.; Culfaz-Emecen, P. Z.; Asatekin, A. Extremely fouling resistant zwitterionic copolymer membranes with ∼ 1nm pore size for treating municipal, oily and textile wastewater streams. *J. Membr. Sci.* **2017**, *543*, 184−194.

(42) Govinna, N.; Kaner, P.; Ceasar, D.; Dhungana, A.; Moers, C.; Son, K.; Asatekin, A.; Cebe, P. Electrospun fiber membranes from blends of poly(vinylidene fluoride) with fouling-resistant zwitterionic copolymers. *Polym. Int.* **2018**, DOI: 10.1002/pi.5578. in press

(43) Kolewe, K. W.; Dobosz, K. M.; Rieger, K. A.; Chang, C.-C.; Emrick, T.; Schiffman, J. D. Antifouling Electrospun Nanofiber Mats Functionalized with Polymer Zwitterions. *ACS Appl. Mater. Interfaces* **2016**, *8*, 27585−27593.

(44) Georgiev, G. S.; Kamenska, E. B.; Vassileva, E. D.; Kamenova, I. P.; Georgieva, V. T.; Iliev, S. B.; Ivanov, I. A. Self-assembly, anti

DOI: 10.1021/acsami.8b03268
ACS Appl. Mater. Interfaces XXXX, XXX, XXX−XXX

polyelectrolyte effect, and nonbiofouling properties of polyzwitterions. *Biomacromolecules* **2006**, *7*, 1329−1334.

(45) Lalani, R.; Liu, L. Synthesis, characterization, and electrospinning of zwitterionic poly(sulfobetaine methacrylate). *Polymer* **2011**, *52*, 5344−5354.

(46) Lalani, R.; Liu, L. Electrospun Zwitterionic Poly(Sulfobetaine Methacrylate) for Nonadherent, Superabsorbent, and Antimicrobial Wound Dressing Applications. *Biomacromolecules* **2012**, *13*, 1853−1863.

(47) Liu, L. Non-adhesive, water-absorbent wound dressing comprising polymerized zwitterionic monomers, where monomer includes sulfobetaine methacrylate, carboxybetaine methacrylate, carboxybetaine acrylamide or poly(phosphoryl)choline. U.S. Patent 2013190672 A1, Jul 25, 2013 A61L-015/24 201350.

(48) Brown, R. H.; Hunley, M. T.; Allen, M. H.; Long, T. E. Electrospinning zwitterion-containing nanoscale acrylic fibers. *Polymer* **2009**, *50*, 4781−4787.

(49) Ye, S.-H.; Hong, Y.; Sakaguchi, H.; Shankarraman, V.; Luketich, S. K.; D'Amore, A.; Wagner, W. R. Nonthrombogenic, Biodegradable Elastomeric Polyurethanes with Variable Sulfobetaine Content. *ACS Appl. Mater. Interfaces* **2014**, *6*, 22796−22806.

(50) Unnithan, A. R.; Ghavami Nejad, A.; Sasikala, A. R. K.; Thomas, R. G.; Jeong, Y. Y.; Murugesan, P.; Nasseri, S.; Wu, D.; Park, C. H.; Kim, C. S. Electrospun zwitterionic nanofibers with in situ decelerated epithelialization property for non-adherent and easy removable wound dressing application. *Chem. Eng. J.* **2016**, *287*, 640−648.

(51) Seo, J.; Seo, J.-H. Fabrication of an Anti-Biofouling Plasma-Filtration Membrane by an Electrospinning Process Using Photo-Cross-linkable Zwitterionic Phospholipid Polymers. *ACS Appl. Mater. Interfaces* **2017**, *9*, 19591−19600.

(52) Heath, D. E.; Cooper, S. L. Design and characterization of sulfobetaine-containing terpolymer biomaterials. *Acta Biomater.* **2012**, *8*, 2899−2910.

(53) Ehrmann, M.; Muller, R.; Galin, J. C.; Bazuin, C. G. Statistical n-Butyl Acrylate-(Sulfopropy1)ammonium Betaine Copolymers. 4. Dynamic Mechanical Properties. *Macromolecules* **1993**, *26*, 4910−4918.

(54) Mori, S.; Barth, H. G. *Size Exclusion Chromatography*; Springer: Heidelberg, Germany, 2013.

(55) Yang, Q.; Li, Z.; Hong, Y.; Zhao, Y.; Qiu, S.; Wang, C.; Wei, Y. Influence of solvents on the formation of ultrathin uniform poly(vinyl pyrrolidone) nanofibers with electrospinning. *J. Polym. Sci., Part B: Polym. Phys.* **2004**, *42*, 3721−3726.

(56) Koombhongse, S.; Liu, W.; Reneker, D. H. Flat polymer ribbons and other shapes by electrospinning. *J. Polym. Sci., Part B: Polym. Phys.* **2001**, *39*, 2598−2606.

(57) Gupta, P.; Elkins, C.; Long, T. E.; Wilkes, G. L. Electrospinning of linear homopolymers of poly(methyl methacrylate): exploring relationships between fiber formation, viscosity, molecular weight and concentration in a good solvent. *Polymer* **2005**, *46*, 4799−4810.

(58) Arinstein, A.; Zussman, E. Postprocesses in tubular electrospun nanofibers. *Phys. Rev. E: Stat., Nonlinear, Soft Matter Phys.* **2007**, *76*, 056303.

(59) Pai, C.-L.; Boyce, M. C.; Rutledge, G. C. Morphology of Porous and Wrinkled Fibers of Polystyrene Electrospun from Dimethylformamide. *Macromolecules* **2009**, *42*, 2102−2114.

(60) Qin, X.-H.; Yang, E.-L.; Li, N.; Wang, S.-Y. Effect of different salts on electrospinning of polyacrylonitrile (PAN) polymer solution. *J. Appl. Polym. Sci.* **2007**, *103*, 3865−3870.

(61) Kim, S. J.; Lee, C. K.; Kim, S. I. Effect of ionic salts on the processing of poly(2-acrylamido-2-methyl-1-propane sulfonic acid) nanofibers. *J. Appl. Polym. Sci.* **2005**, *96*, 1388−1393.

(62) Grassl, B.; Francois, J.; Billon, L. Associating behaviour of polyacrylamide modified with a new hydrophobic zwitterionic monomer. *Polym. Int.* **2001**, *50*, 1162−1169.

(63) Schulz, D. N.; Peiffer, D. G.; Agarwal, P. K.; Larabee, J.; Kaladas, J. J.; Soni, L.; Handwerker, B.; Garner, R. T. Phase behaviour and solution properties of sulphobetaine polymers. *Polymer* **1986**, *27*, 1734−1742.

(64) Rehm, T. H.; Schmuck, C. Ion-pair induced self-assembly in aqueous solvents. *Chem. Soc. Rev.* **2010**, *39*, 3597−3611.

(65) Bredas, J. L.; Chance, R. R.; Silbey, R. Head Head Interactions in Zwitterionic Associating Polymers. *Macromolecules* **1988**, *21*, 1633−1639.

(66) Shao, Q.; Jiang, S. Molecular Understanding and Design of Zwitterionic Materials. *Adv. Mater.* **2015**, *27*, 15−26.

(67) Doshi, J.; Reneker, D. H. Electrospinning process and applications of electrospun fibers. *J. Electrost.* **1995**, *35*, 151−160.

(68) Liu, Y.; He, J.-H.; Yu, J.-y.; Zeng, H.-m. Controlling numbers and sizes of beads in electrospun nanofibers. *Polym. Int.* **2008**, *57*, 632−636.

(69) Beamson, G.; Briggs, D. *High Resolution XPS of Organic Polymers: The Scienta ESCA300 Database*; Wiley: Chichester, England, 1992; p 295.

(70) López, G. P.; Castner, D. G.; Ratner, B. D. XPS O 1s binding energies for polymers containing hydroxyl, ether, ketone and ester groups. *Surf. Interface Anal.* **1991**, *17*, 267−272.

DOI: 10.1021/acsami.8b03268
ACS Appl. Mater. Interfaces XXXX, XXX, XXX−XXX